

Expression of the mitotic kinesin Kif15 in postmitotic neurons: Implications for neuronal migration and development

DANIEL W. BUSTER¹, DOUGLAS H. BAIRD¹, WENQIAN YU¹, JOANNA M. SOLOWSKA¹, MURIEL CHAUVIÈRE², AGNIESZKA MAZUREK^{1,3}, MICHEL KRESS² and PETER W. BAAS^{1,*}

¹Department of Neurobiology and Anatomy, Drexel University College of Medicine, Philadelphia, PA 19129, USA;

²IFC1, UPR 9044 CNRS, Villejuif, France; ³Gliwice, Poland

Peter.W.Baas@drexel.edu

Received 15 April 2003; accepted 10 July 2003

Abstract

Kif15 is a kinesin-related protein whose mitotic homologues are believed to crosslink and immobilize spindle microtubules. We have obtained rodent sequences of Kif15, and have studied their expression and distribution in the developing nervous system. Kif15 is indeed expressed in actively dividing fibroblasts, but is also expressed in terminally postmitotic neurons. In mitotic cells, Kif15 localizes to spindle poles and microtubules during prometaphase to early anaphase, but then to the actin-based cleavage furrow during cytokinesis. In interphase fibroblasts, Kif15 localizes to actin bundles but not to microtubules. In cultured neurons, Kif15 localizes to microtubules but shows no apparent co-localization with actin. Localization of Kif15 to microtubules is particularly good when the microtubules are bundled, and there is a notable enrichment of Kif15 in the microtubule bundles that occupy stalled growth cones and dendrites. Studies on developing rodent brain show a pronounced enrichment of Kif15 in migratory neurons compared to other neurons. Notably, migratory neurons have a cage-like configuration of microtubules around their nucleus that is linked to the microtubule array within the leading process, such that the entire array moves in unison as the cell migrates. Since the capacity of microtubules to move independently of one another is restricted in all of these cases, we propose that Kif15 opposes the capacity of other motors to generate independent microtubule movements within key regions of developing neurons.

Introduction

Neurons are terminally postmitotic cells that undergo dramatic changes in motility and morphology during embryonic development. Many neurons are born far from their ultimate destinations and migrate over substantial distances prior to the extension of axons and dendrites (Hatten, 1999). Migration typically occurs by movement of the cell body behind a short leading process. After the cell body becomes stationary, the neuron extends a bona fide axon, whose tip is a highly motile structure termed the growth cone which forages over potentially long distances to find its target. These various changes in motility and morphology are intimately associated with changes in microtubule configuration. During migration, microtubules surrounding the nucleus are somehow linked with those within the leading process, such that the entire microtubule array moves as a unit, thus dragging the cell body (Rivas &

Hatten, 1995; Feng & Walsh, 2001). However, after the cell body becomes stationary, individual microtubules move freely from the cell body down the length of the axon to promote its rapid elongation (Ahmad *et al.*, 1998; Slaughter *et al.*, 1997; Wang & Brown, 2002). In some cases, growth cones can stall, and when they do, they are occupied by a tightly bundled loop of microtubules that displays no movement (Dent *et al.*, 1999). Microtubules are also transported into dendrites (Sharp *et al.*, 1995), but their transport is severely dampened compared to the situation in the axon, accounting in part for the short length of the dendrite (Yu *et al.*, 2000).

Microtubules are configured during neuronal development by a variety of factors which include forces generated by molecular motor proteins. These forces transport microtubules from the cell body into developing axons and dendrites (Ahmad *et al.*, 1998; Sharp

*To whom correspondence should be addressed.

et al., 1995; Wang & Brown, 2002), into newly developing branches and sprouts (Yu *et al.*, 1994, 1996), and from the growth cone outward (Dent *et al.*, 1999). Cytoplasmic dynein appears to be the principle motor involved in transporting neuronal microtubules (Dillman *et al.*, 1996; Ahmad *et al.*, 1998), but a variety of kinesin-related motors appear to play crucial roles as well. Our studies suggest that CHO1/MKLP1 is essential for transporting microtubules into dendrites (Sharp *et al.*, 1997), and that Eg5 may be important for configuring microtubules in regions of new growth (Ferhat *et al.*, 1998). Interestingly, these motors were previously thought to be mitosis-specific and have known functions in generating forces on spindle microtubules (Sharp *et al.*, 2000). Migrating neurons also rely on cytoplasmic dynein and associated molecules such as LIS1 and doublecortin for the organization and movement of the microtubule array (Smith *et al.*, 2000; Wynshaw-Boris & Gambello, 2001). However, to date, no molecule has yet been identified that is particularly enriched in dendrites, stalled growth cones, and migratory neurons that has the appropriate properties to crosslink the microtubules such that other motors are less able to move them independently of one another. In the mitotic spindle, motor activities are often opposed by other motors (Sharp *et al.*, 2000). Might neurons express a motor that tethers microtubules and opposes their potential movement by other motors?

A kinesin-related protein termed Kif15 is an attractive candidate. Studies on the Kif15 homologues, KRP180 and Xklp2, in mitotic cells show that their forces are required to maintain the separation of spindle poles after they are separated by homologues of CHO1/MKLP1 and Eg5 (Rogers *et al.*, 2000; Sharp *et al.*, 2000; Wittmann *et al.*, 2000). Thus, the forces generated by Kif15 appear to be important not for moving microtubules apart but for crosslinking neighboring microtubules and opposing their movement by other motors. Such a function would be ideally suited for tethering together microtubules in migratory neurons, stalled growth cones, and developing dendrites to oppose their capacity to move freely and independently of one another. To investigate this possibility, we have now obtained the sequences for rat and mouse KIF15, and have studied the expression and distribution of this motor within developing neurons and brains.

Materials and methods

Kif15 SEQUENCING AND PREPARATION OF PROBES

RT-PCR was used to obtain complete sequences of Kif15 from whole mouse day 13–14 embryos, rat neonatal whole brain tissue, and cultured rat lung fibroblasts (ATCC designation RFL-6). Total RNA was obtained after tissue disruption with Tri Reagent (according to manufacturer's instructions, Sigma) and isopropanol precipitation. cDNA was generated

from total RNA using an oligo-dT₍₁₅₎ primer and Powerscript reverse transcriptase (Clontech) according to manufacturer's instructions.

PCR primer sequences were based primarily on available mouse and human Kif15 sequences, and rat EST sequence information. Alignments identified regions of identical or highly similar nucleotide sequence that were selected as annealing sites for primers. PCR products were ligated into TA cloning vectors (Qiagen, Invitrogen), and then sequenced on an ABI Prism DNA Sequencer 377. Sufficient independent clones were sequenced to provide at least three reads of all coding cDNA of Kif15.

Anti-Kif15 polyclonal antibodies were generated by immunizing rabbits with either purified recombinant GST-Kif15 stalk 1 (human KLP2 amino acids 367–1161) or purified recombinant GST-Kif15 stalk 2 (human KLP2 amino acids 1162–1389). Kif15-specific antibodies were obtained by pre-absorbing rabbit serums with GST protein to deplete GST-specific antibodies, then incubating the clarified serums with either SDS-PAGE purified GST-stalk 1 or GST-stalk 2 antigens bound to PVDF. For some experiments, results were confirmed using two different monoclonal antibodies generated against the Kif15 stalk 2 domain.

Sense and anti-sense riboprobes were synthesized with a DIG RNA labeling kit (Boehringer Mannheim). Template for the production of non-radioactive riboprobes for Northern blotting and *in situ* hybridization was made by subcloning a 1676bp fragment (corresponding to Kif15 nucleotides 1034 to 2709) into pBluescript SK-plasmid (Stratagene). After template linearization, "run-off" sense and antisense digoxigenin-labelled riboprobes were transcribed with a ribonucleotide mix containing digoxigenin-UTP (Roche) and either T3 or T7 RNA polymerase (Promega) according to manufacturer's instructions.

WESTERN BLOTTING

Various regions of brain were dissected from Sprague-Dawley rat fetuses and postnatal pups, washed with cold PBS and then stored in liquid nitrogen. Sympathetic ganglia were dissected from fetuses and pups as described by He and Baas (2003) and stored in liquid nitrogen. Thawed tissues were disrupted with a chilled Dounce glass homogenizer in 4 volumes (4 mls buffer/g tissue) cold lysis buffer (60 mM Pipes [piperazine-N,N'-bis-2-ethanesulfonic acid], 25 mM Hepes [N-2-hydroxyethylpiperazine-N'-2-ethanesulfonic acid], pH 6.9, 100 mM NaCl, 10 mM EGTA [ethyleneglycol tetraacetic acid], 2 mM MgCl₂, 2 mg/ml TAME [tosyl-L-arginine methyl ester], 2 ug/ml pepstatin and leupeptin, 4 ug/ml aprotinin, 0.5 mM PMSF [phenylmethylsulfonyl fluoride], 10 mM 2-mercaptoethanol, 0.1% TX-100). Cultured RFL-6 fibroblasts were washed with PBS and extracted with cold lysis buffer. Fibroblast extracts and brain homogenates were centrifuged at 15 K × g for 30 minutes at 4°C, and supernatants were mixed with Laemmli sample buffer (Sambrook *et al.*, 1989), boiled, and stored at –20°C. SDS-PAGE and electroblotting were performed according to established procedures (Sambrook *et al.*, 1989). Blots were blocked with Blotto (5% [w/v] powdered non-fat milk, 10% [v/v] glycerol, 0.05% [v/v] Tween-20, 0.05% [w/v] thimerosal in PBS), probed with 1/2000 anti-Kif15 polyclonal in Blotto, washed, and reprobed with 1/500 goat anti-rabbit IgG

HRP conjugate (Sigma) in Blotto. Blots were developed by chemiluminescence (Amersham).

PREPARATION AND IMMUNOSTAINING OF CELL CULTURES

Cultures of rat sympathetic neurons were prepared as previously described (He & Baas, 2003). Neurons were plated onto polylysine-treated glass coverslips overnight and then exposed to either laminin or matrigel (Yu *et al.*, 2001). Cultures of rat fibroblasts (RFL-6) were maintained in 80% F12K medium (BD Biosciences)/20% fetal bovine serum (Hyclone) and were prepared for immunofluorescence and pharmacologic studies by subculturing on untreated glass coverslips submerged in culture dishes. For fixation, cells were briefly washed with 37°C PBS, and then submerged in 100% methanol at -20°C for 6 minutes. We found that methanol fixation, but not 4% paraformaldehyde/0.1% glutaraldehyde fixation, preserved Kif15 co-localization with the cytoskeleton in RFL-6 and sympathetic neurons. After fixing, cells were washed with PBS/0.1% Tween-20, blocked with 5% normal goat serum in PBS/0.1% Tween-20 for 30 minutes, and then exposed to Kif15 antibody overnight at 4°C. Samples were rinsed three times for 5 minutes each in PBS. In some experiments, cells were then exposed for 1 hr at 37°C to a solution containing an anti- α -tubulin monoclonal antibody conjugated directly to Cy3 (Sigma; 1:100) together with an FITC-conjugated secondary goat anti-rabbit secondary antibody (Jackson ImmunoResearch; 1:100). In other experiments, cells were exposed in a similar fashion to a solution containing an anti-actin monoclonal antibody conjugated directly to FITC (Sigma; 1:100) together with a Cy3-conjugated goat anti-rabbit secondary antibody (Jackson ImmunoResearch; 1:100). Cells were then rinsed extensively in PBS, and mounted in a medium that reduces photobleaching. Photographs were obtained using a Pascal Confocal Microscope (Zeiss) with the pinhole set to obtain optical sections with a thickness of 1–2 μ m. FITC and Cy3 images were obtained sequentially rather than simultaneously to eliminate the potential for bleed-through between channels. Zeiss Axiovision and Adobe Photoshop software were used to capture and process digital images.

For some immunostaining experiments, microtubules or F-actin were disassembled prior to fixation. To disassemble microtubules, cultures were incubated with 2 μ g/ml nocodazole (Sigma) for 1 hr. To disassemble F-actin, cultures were incubated for 30 minutes with latrunculin (Molecular Probes) used at concentrations ranging from 0.02 to 2 μ g/ml.

IMMUNOSTAINING AND *IN SITU* HYBRIDIZATION OF BRAIN SECTIONS

Sections of mouse brain at various stages of development were prepared for single-label visualization of Kif15 immunoreactivity using a standard peroxidase technique, and for double-label immunofluorescence using the Kif15 polyclonal antibody together with a monoclonal antibody against β III-tubulin (TUJ1, BAbCO). For single-label studies, sections were treated with 0.2% H₂O₂ in TBST (10 mM Tris-HCl, pH 7.5, 150 mM NaCl, 0.1% Tween-20), blocked with 5% skim milk in TBS and incubated overnight with Kif15 antibody (1:5000), followed by an anti-rabbit secondary conjugated

with biotin (Jackson ImmunoResearch; 1:400) for 2 hrs, then incubated with avidin-biotin peroxidase complex (Vectastain Elite ABC Kit, Vector Lab.). HRP activity was detected using 0.5 mg/ml diaminobenzidine (DAB), 0.006% H₂O₂, and 0.1% nickel ammonium sulfate in 50 mM Tris, pH 7.5. Sections for double immunofluorescence staining were permeabilized with 0.2% Triton X-100, blocked with 5% normal goat serum, incubated overnight with antibodies against KIF-15 (1:500) and TUJ1 (1:200), and then incubated for 2 hrs with secondary antibodies: anti-rabbit conjugated with Cy3 and anti-mouse conjugated with FITC (both: 1:200; Jackson ImmunoResearch). Fluorescently labeled sections were imaged using the Pascal confocal microscope as described above, while histochemically-labeled sections were imaged using a Zeiss 135TV inverted microscope equipped with a high resolution cooled CCD camera (NU200, Photometrics). For *in situ* hybridization, frozen sections (16–20 μ m) were collected and *in situ* hybridized for 21 hrs at 55°C in a humid chamber using 200 ng/ml of DIG labeled riboprobes in hybridization buffer containing 50% formamide and 10% dextran sulfate. Sections were then washed in 2 \times SSC at 65°C for 1 hr and in 0.1 \times SSC at 65°C for 1 hr. Hybrids were detected using anti-DIG antibody conjugated with alkaline phosphatase (Boehringer Mannheim).

Results

Kif15 IS A HOMOLOGUE OF THE MITOTIC MOTOR, Xklp2

RT-PCR of total RNA isolated from perinatal rat whole brain revealed the presence of a transcript that shows a high degree of sequence identity with Xklp2 and KRP180. We have chosen to name this putative motor Kif15 based on its strong similarity with a published partial sequence identified in a broad screen for kinesin-like motors in the mouse genome (Nakagawa *et al.*, 1997). Figure 1A shows the complete amino acid sequence of rat neuronal Kif15 that was compiled as a consensus sequence from multiple, independently derived clones obtained by RT-PCR of P0 rat whole brain total RNA. The deduced amino acid sequence predicts a protein of 1385 amino acids with a molecular mass of 159,537 Daltons. Kif15 was also sequenced by RT-PCR from total RNA isolated from mitotically active, cultured rat RFL-6 fibroblast cells. The Kif15 sequences from rat brain and RFL-6 cells are nearly identical throughout their lengths (Fig. 1B), suggesting that the rare differences are due to allelic differences of the particular rat strains and that these two sequences originate from the same gene. We also obtained the complete Kif15 sequence from whole mouse embryos, and it has 95% overall similarity to the rat sequence (Fig. 1B). The high level of similarity between Kif15 and members of the Xklp2 motor subfamily indicates that Kif15 is a new member of this subfamily. Like its mitotic homologues, Kif15 has an N-terminal kinesin-like motor domain followed by an extended region of predicted coiled-coil stalk (Fig. 1C). Kif15 also resembles the other Xklp2

subfamily homologues by having a conserved leucine zipper at the C-terminus of the stalk, and a consensus cyclin-dependent kinase (CDK) phosphorylation site within the stalk whose relative position (residue 661)

is conserved within each homologue (Fig. 1A and B). Interestingly, the Kif15 stalk contains a myosin tail homology domain extending from amino acid residues 740 to 1333 (Fig. 1C). This myosin homology domain

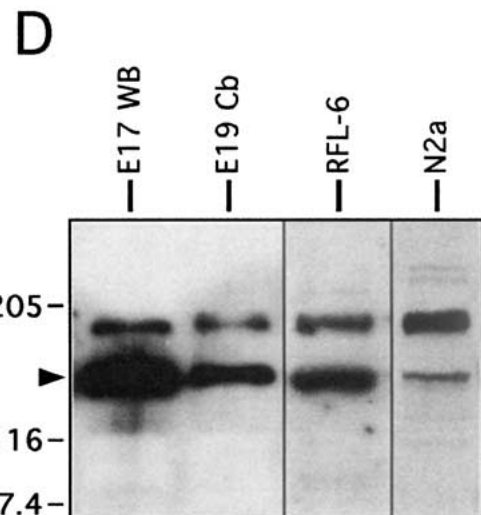
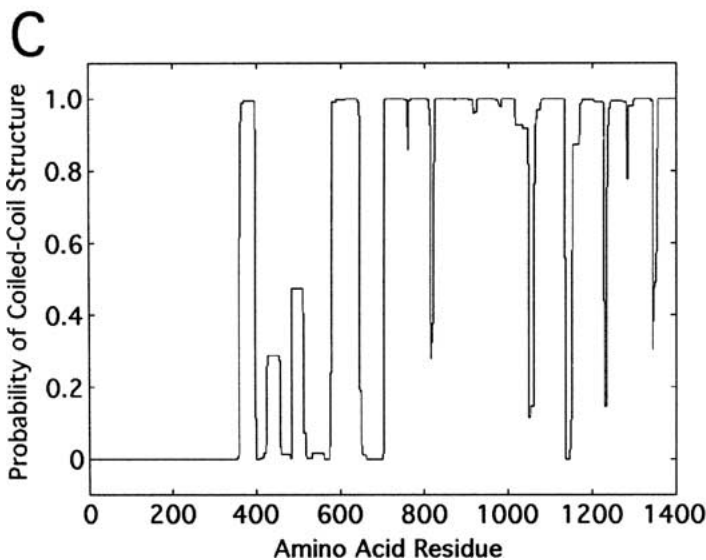
A

MAPGCKSELR	NVTNSHSNP	SNEDDAIKVF	VRIRPAEEGA	RSADGEQSLC	LSVLSQTALR	60
LHSNPDPKTF	VDYVAGMDT	TOESVFSTVA	KSIVESCMSG	YNGTIFAYGQ	TGSGKTFTMM	120
GPSDSDNFESH	NLRGVIPRSF	EYLFSLIDRE	KEKAGAGKSF	LCKCSFIEVY	NEQIYDLLDS	180
ASVGLYLREH	IKKGVFVGA	VEQVVASAAE	AYQVLSRGWR	NRRVASTSMN	RESSRSHAVF	240
TITIESMEKS	SEAVNIRTSL	LNLVLDLAGE	ROKDTHAEGM	RLKEAGNINR	SLSCLGOVIT	300
ALVDVGNQKQ	RHVCYRDSKL	TFLLRDSLGG	NAKTAIIANV	HPGSRCFGET	LSTLNFAQRA	360
KLIKMKAVVN	EDTQGNVSQL	QAEVKRLREQ	LSQFTSQGLT	PGSSLARDKE	KANYMEYFLE	420
AMLFFKKESE	EKKSLEKIT	QLEDLTLKKE	KFIQSNKMIV	KFREDQIMRL	ERLQKEARG	480
FLPEEQDRLL	SELRDEIRTL	REQVEHHPRL	AKYAMENHSL	REENRKLKLL	APVKRAHELD	540
AQAIARLEQA	FSEVSTETN	DIGPQGLPPK	AIKEPSFFTS	TEKLVQQLLQ	IQTELNNSKQ	600
EYEEFKELTR	KKQLELESEL	QSLQKANLNL	ENLEATKVC	KRQEVSQLNK	IHAETLKIIIT	660
T PTKAYQLCS	RLVPKSSPEV	GSFGFLRSQS	APDNDILNEP	VPPEMSEQAL	EAVSEELRTV	720
Q EQLSVLQVK	LDEEHEKLNK	LQQNVDRLRH	HSTQMQLFS	SERSDWSKQQ	QDYLTQLSDL	780
EKQLQDAQTK	NDFLKEVVD	LRIVLNSADK	ELSLVKLEYS	TFKESQEKEL	SQLSDRHVQV	840
QLQLDNARLE	NEKLLESQAC	LQDSYDNLQE	VMKFEVDQLS	KNLQNCQEN	ETLKSDDLHNL	900
VELFEAEKER	NNKLSLQFEE	DKENSSKEIL	KALETVRQEK	QEEMARCEKQ	MAKVQEELES	960
LLAAENVVSC	LEKSRESDE	LVTNLMNQIQ	ELRTSAGEKS	EAITLTKQEL	QDISCKYTAA	1020
VADKEESKEL	IRRQEVILE	LKETLRLRIL	SEDIERDMLC	EDLAHATEQL	NMLTEASKKH	1080
SGLLQSAQEE	LTKKEALIQE	LQHKLNQEKE	EVEQKKSEYN	LKMKQLEHVM	GSAPYPPQSP	1140
KTPPHFQTHL	AKLLETQEQE	IEDGRASKMS	LQHLVTKLNE	DREVKNAEIL	RMKDQLREME	1200
NLRLESQQLR	ERTWLLQTQL	DDMKRQGESS	SQSRPDSQQL	KNEYEEEIIR	ERLAKNKLIE	1260
EMLKMKTDLE	EVQSALDSKE	KFCHRMSEEV	ERTRTLESRA	FQEKEQLRSK	LEEMYEERER	1320
TCQEMEMLRK	QLEFLAEENG	KLIGHQNLHQ	KIQYVVRLLK	ENIRLAEETE	KLRAENVFLK	1380
ERKKE						1385

B

Percent amino acid identity (similarity)

	Motor	P _V	Coil I	Coil II
KIF15 (rat brain)	370aa		759aa	256aa
KIF15 (RFL-6)	100		99 (99)	99 (99)
KIF15 (mouse)	98 (98)		92 (95)	90 (93)
HKLP2	93 (94)		82 (87)	83 (89)
XKLP2	82 (89)		55 (67)	46 (59)



is similar to the domain present in the kinesin motor, KhcU, and is responsible for interaction with the actin-based motor, MyoVA (Huang *et al.*, 1999).

Western blotting of clarified rat brain lysates using either of two different affinity-purified polyclonal antibodies raised against separate regions of the stalk of the human Kif15 homologue, Hk1p2, identified two immunoreactive bands with apparent molecular weights of 157 and 188kD (Fig. 1D). The 157kD band is not surprising because a similar mass is predicted from the Kif15 amino acid sequence. Bands of these same two molecular weights were obtained with Western blotting of whole brain, various parts of the brain such as cerebellum, RFL-6 cells, and of various cultured mouse cells, including neuroblastoma Neuro-2a cells. No evidence for splice variants was found in the PCR search, and only one band was visualized by Northern blot analysis of mouse RNA probed with a Kif15 riboprobe (not shown). Specificity of the anti-Kif15 antibodies is supported by the observation that, besides the results obtained with two polyclonal antibodies, two different monoclonal antibodies raised against stalk 2 of Kif15 (see Methods) produced similar results, with the same two bands appearing on Western blots (data not shown). Given that four different Kif15 antibodies recognize both bands on Western blots, we conclude that the upper band is a modified variant of Kif15 with slower mobility. Antibody specificity is further supported by the fact that Kif15 immunoreactivity is absent from cultured fibroblasts treated with Kif15-specific siRNA (M. Kress, unpublished observations).

DISTRIBUTION OF Kif15 DURING THE CELL CYCLE OF DIVIDING CELLS

The Kif15 homologues, Hk1p2, KRP180 and Xk1p2, have been shown to concentrate on spindle poles and microtubules in mitotic HeLa cells, sea urchin eggs, and XL177 cells (Boleti *et al.*, 1996; Rogers *et al.*, 2000;

Sueishi *et al.*, 2000). Localization to these structures is expected, given that the activities of these mitotic Kif15 homologues are required to maintain the bipolar structure of the spindle and prevent collapse to a monastral spindle (Rogers *et al.*, 2000; Wittmann *et al.*, 2000). Immunostaining mitotic RFL-6 rat cells with the anti-Kif15 polyclonal antibodies produced a staining pattern in pre-anaphase cells that is very similar to published images (Boleti *et al.*, 1996; Rogers *et al.*, 2000; Sueishi *et al.*, 2000). Kif15 immunostaining in RFL-6 cells in mitotic stages prior to anaphase is concentrated on the spindle poles and microtubules (Fig. 2A and B). Interestingly, after metaphase, Kif15 immunostaining of spindle microtubules decreased, but increased at the sites of invaginating cell membranes—a position that corresponds to the location of the contractile actomyosin ring of dividing cells (Fig. 2C and D). Indeed, these sites of Kif15 enrichment co-localized with actin immunoreactivity in late mitotic RFL-6 cells (Fig. 2E and F). A similar cortical staining for the sea urchin homologue of Kif15 was observed during late phases of mitosis in sea urchin zygotes (G. Rogers, personal communication). The centrosomes continued to stain for Kif15 in late mitotic stages (Fig. 2D, arrows).

We next examined Kif15 immunostaining during interphase, a stage of the cell cycle not studied in detail in previous work on the Kif15 homologues. Other than the centrosome (Fig. 3C, arrow), there is no detectable overlap in the staining of Kif15 and microtubules in interphase RFL-6 cells. In approximately 45% of interphase cells, Kif15 immunostaining had a variegated filamentous appearance, but the filaments did not coalign with microtubules. This was particularly obvious in the merged images in Fig. 3A–C, where the microtubules are observed to extend well beyond the Kif15 staining, which falls short of the cell periphery. Except for the fact that the Kif15 staining did not extend to the periphery, its appearance was very similar to that of actin filaments and bundles (Fig. 3D). Even though the Kif15 sequence lacks any canonical nuclear localization signal, Kif15

Fig. 1. Rat brain Kif15 sequence and predicted secondary structure. (A) Deduced amino acid sequence of rat brain Kif15. Underlined sequence corresponds to the kinesin-like motor domain determined by alignment with other kinesin-like motors (<http://mc11.mcri.ac.uk/khome/>). Underlined and italicized sequences are leucine zipper motifs (<http://psort.nibb.ac.jp/>). Shaded sequence marks a potential PEST sequence (<http://www.at.embnet.org/embnet/tools/bio/PESTfind/>). The boxed threonine is a consensus phosphorylation site for cyclin-dependent kinase (CDK). (B) Percent amino acid sequence identity (similarity) of rat brain Kif15 domains compared to RFL-6 Kif15, mouse Kif15, human Hk1p2 (GenBank accession number AB035898), and *Xenopus* Xk1p2 (accession number X94082). The stalk was analyzed as two discrete domains; Coil 2 corresponds to the “tail” as defined by Boleti *et al.* (1996). The conserved consensus CDK phosphorylation site is marked by “P”. The conserved leucine zipper location is indicated by the shaded region in Coil 2. (C) Lupas plot showing the probability of coiled-coil secondary structure as a function of position along Kif15 (http://www.ch.embnet.org/software/COILS_form.html). The location of a myosin tail homology domain was found using the NCBI Conserved Domain Database (<http://www.ncbi.nlm.nih.gov/Structure/cdd/cddsrv.cgi?uid=pfam01576>) and is indicated by shading. (D) Western blot of clarified lysates generated from rat E17 whole brain (E17 WB), rat E19 cerebellum (E19 Cb), cultured rat RFL-6 cells, and cultured mouse N2a neuroblastoma cells. Molecular weight markers (in kD) are shown to the left. The arrowhead indicates a band corresponding to the calculated size of the deduced amino acid sequence. These sequence data are available from GenBank/EMBL/DBJ under accession numbers KIF15: AY291580 (rat brain), KIF15: AY291581 (RFL-6), and KIF15: NML181635 (mouse embryo).

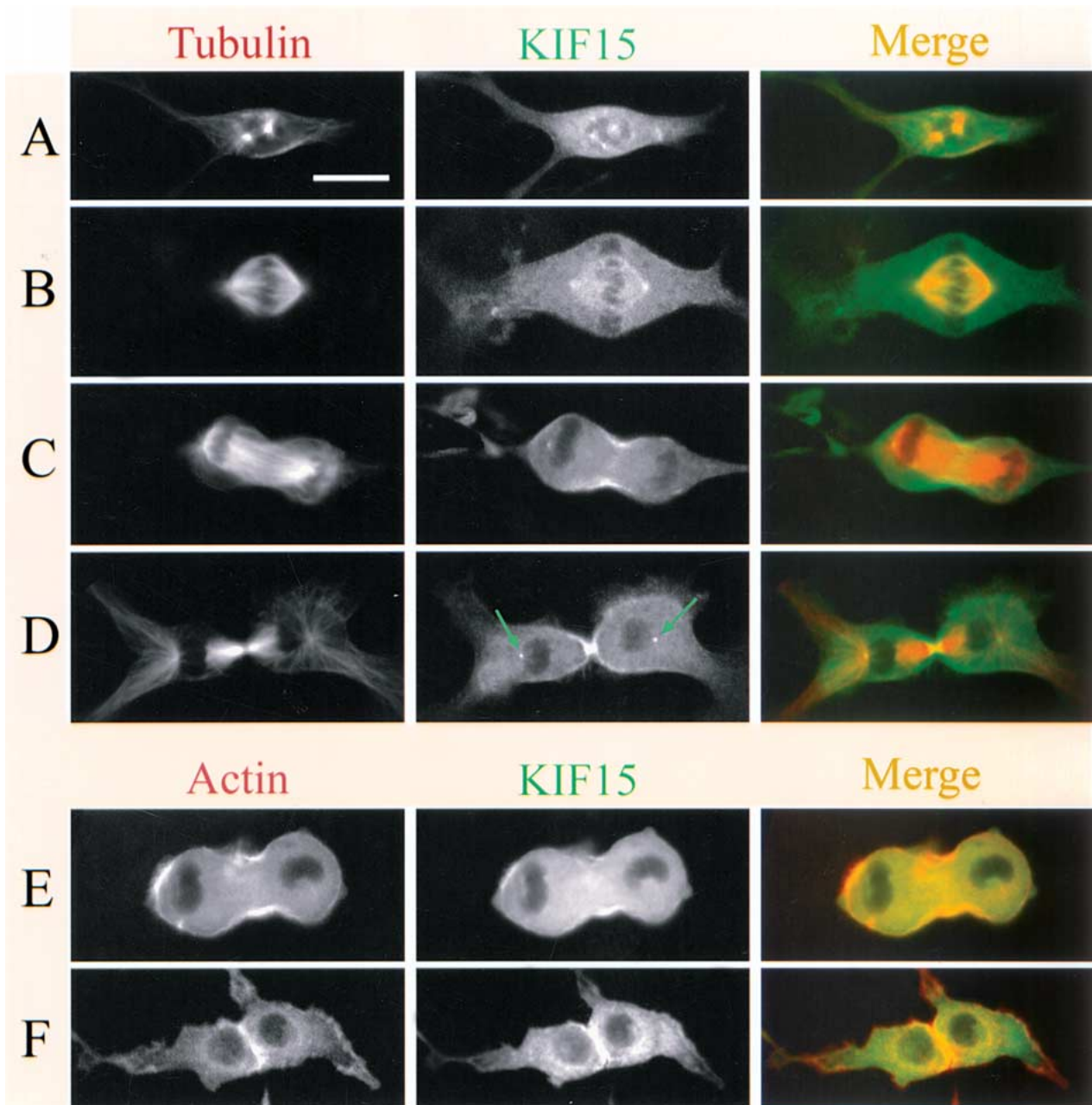


Fig. 2. Kif15 co-localizes with microtubules in early mitotic RFL-6 rat fibroblasts. Representative examples of cultured RFL-6 cells in prometaphase (A), near metaphase (B), late anaphase/early cytokinesis (C), and late cytokinesis (D) were probed with antitubulin (first column) and anti-Kif15 (second column) antibodies (anti-Kif15 stalk 1 staining shown in this and subsequent figures). The merged images (third column) display microtubules pseudocolored red, Kif15 pseudocolored green, and regions of overlay as yellow. The arrows in D indicate the immunopositive spindle poles. E, F. Cytokinetic RFL-6 cells probed with anti-actin (first panel), anti-Kif15 (second panel), and the merged images in the last panel (actin displayed in red, Kif15 in green, overlay regions in yellow). Kif15 co-localizes with microtubules during the early stages of mitosis, and with actin (but not microtubules) in the later stages. Bar, 20 μ m.

immunoreactivity was frequently noted in the nuclei of the cells.

DISTRIBUTION OF Kif15 IN CULTURED SYMPATHETIC NEURONS

Neurons plated on a polylysine substrate produce either only lamellae or relatively short, slow-growing

nascent axons. Being particularly flat, the lamellae afford the best opportunity to assess the potential co-localization of Kif15 with individual microtubules. As shown in Figure 4A, Kif15 immunoreactivity aligns with many, but not all, microtubules within the lamella. When short axons are extended, they contain a dense bundle of microtubules that traverses most of the length of the process (Fig. 4B). The bundle in the distal region

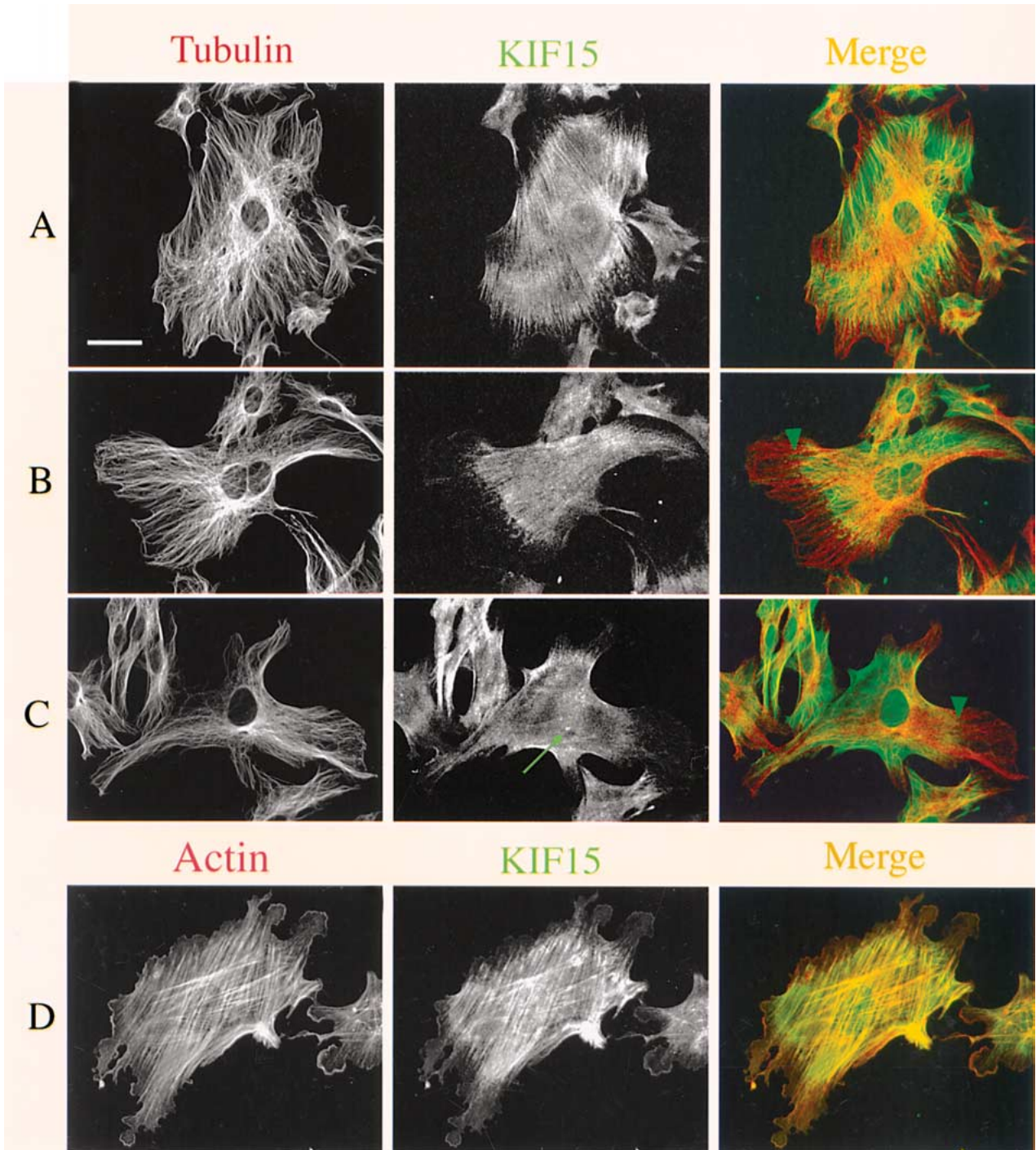


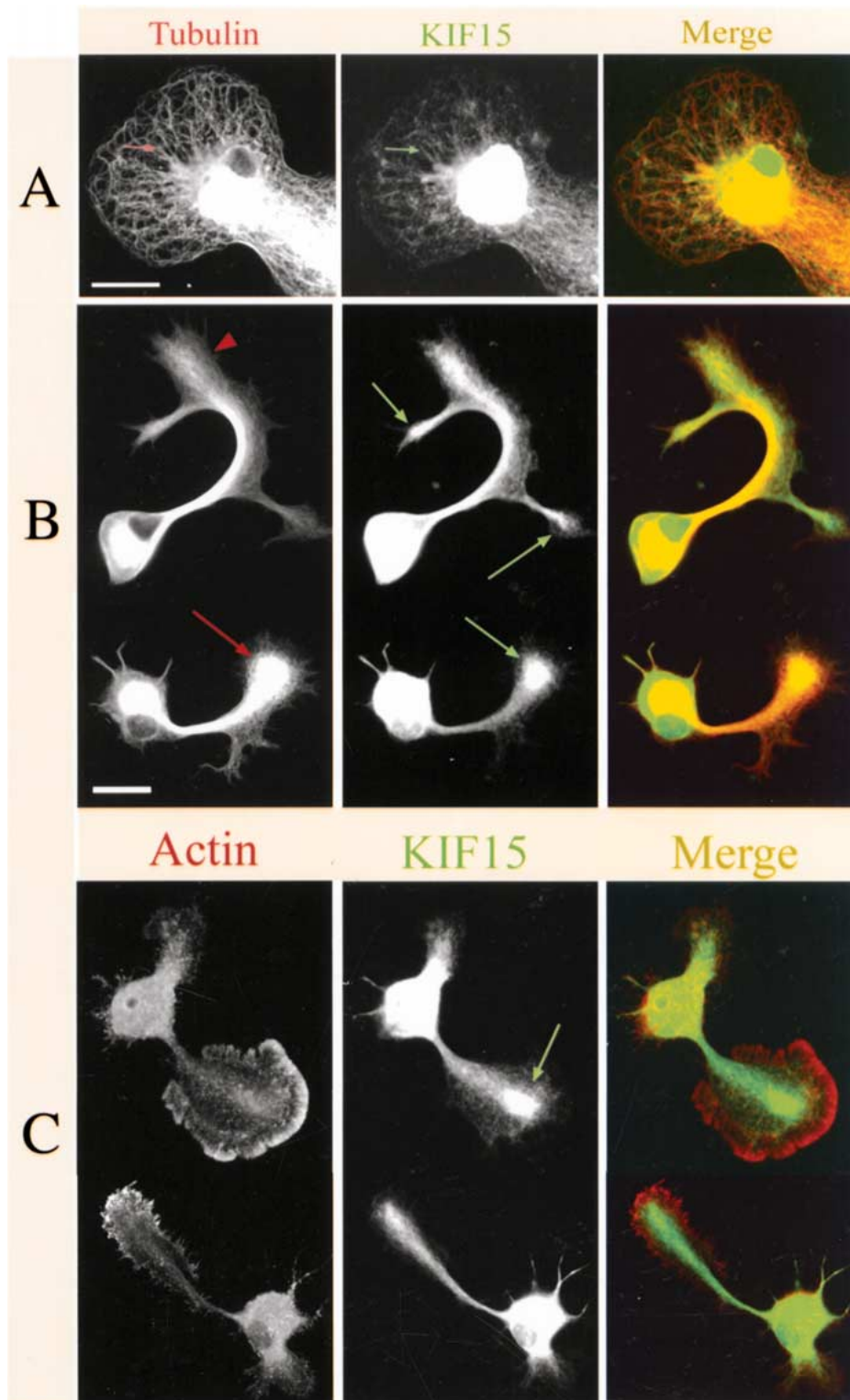
Fig. 3. Kif15 co-localizes with actin fibers in interphase RFL-6 rat fibroblasts. (A–C) RFL-6 cells probed with anti-tubulin (first column), and anti-Kif15 (second column) antibodies. Merged images are shown in the third column (tubulin in red, Kif15 in green, overlay in yellow). The arrowheads in B, C (last panel) indicate an apparent boundary to the limit of Kif15 immunostaining that does not extend to the cell periphery. The arrow in C indicates presumptive centrosome staining by Kif15 antibody (two centrioles can be resolved). (D) RFL-6 cell immunostained with actin (first column), Kif15 (second column), and the merged image shown in the last column (actin in green, Kif15 in red, overlay in yellow). Kif15 shows no apparent co-localization with microtubules during interphase, but shows a tight co-localization with actin.

of the axon alternates between a splayed array of microtubules (left panel, Fig. 4B, arrowhead) and a particularly dense knot of tightly packed microtubules (left panel, Fig. 4B, arrow) which higher resolution stud-

ies have revealed to consist of curved microtubules that loop back on themselves (Dent *et al.*, 1999; Yu *et al.*, 2001). Correlative imaging studies have shown that looped bundles appear within growth cones that

are “stalled” in their advance while splayed arrays appear in growth cones that are advancing forward (Dent *et al.*, 1999; Yu *et al.*, 2001). The Kif15 immunostaining generally, if not perfectly, overlaps with the microtubule array, and the co-localization is particularly good in regions where the microtubules bundle together.

Interestingly, Kif15 immunostaining is typically very high in the area of the dense knot of microtubules in stalled growth cones compared to other regions of the bundle (see arrows), suggesting that looped bundles are richer yet in Kif15 than paraxial bundles. Unlike interphase RFL-6 cells, there is no



detectable co-localization of Kif15 with actin in neurons (Fig. 4C).

Rat sympathetic neurons plated on polylysine-coated dishes and then subsequently treated for 2 hrs with either matrigel (Fig. 5A) or laminin (Fig. 5B and C) respond to these growth factors by extending thinner, more complex axons that grow at rapid rates (Rivas *et al.*, 1992; Slaughter *et al.*, 1997; Tang & Goldberg, 2000; Yu *et al.*, 2001). As with the cells plated on polylysine alone, there is good overlap between microtubules and Kif15 in most regions of the neuron, with particularly good overlap in regions of high microtubule density, which possibly indicate regions of microtubule bundling. It was not possible to determine if neuronal centrosomes are stained with Kif15 antibody due to the intense immunofluorescence within the soma. Neuronal nuclei frequently displayed a heterogeneous Kif15 immunofluorescence (Figs. 4 and 5, middle panels).

PHARMACOLOGIC STUDIES ON THE POTENTIAL ASSOCIATION OF Kif15 WITH MICROTUBULES AND F-ACTIN

The observations thus far suggest that Kif15 associates either with microtubules or F-actin at different cell cycle stages, and that terminally postmitotic neurons display a Kif15-microtubule association that is characteristic of early mitotic fibroblasts rather than the F-actin association characteristic of late mitosis and interphase. One possibility is that Kif15 truly switches affinity from one filament system to the other, while another possibility is that Kif15 may associate with the more abundant cytoskeletal filament system. To explore this issue, we ascertained the distribution of Kif15 in both RFL-6 cells and in sympathetic neurons after treatment with drugs that depolymerize either F-actin or microtubules. A relatively low dose of latrunculin (0.02 $\mu\text{g}/\text{ml}$) did not detectably alter the morphology of the RFL-6 cells, but caused a loss of the unbundled splayed actin filaments and an apparent increase in the thickness or staining of the actin bundles (Fig. 6A). Under these

conditions, Kif15 showed a very tight co-localization with the actin bundles in virtually every cell examined. A higher dose of latrunculin (0.2 $\mu\text{g}/\text{ml}$) caused the lamellae of RFL-6 cells to collapse into narrow processes (Fig. 6B). This alteration in morphology has been reported previously for fibroblastic cells treated with actin-depolymerizing agents (see for example, Haendel *et al.*, 1996). In these cells, Kif15 continued to show a tight co-localization with the remaining small patches of actin (see arrow). The actin immunostaining, Kif15 immunostaining, and cellular morphology all remained essentially unchanged after treatment with 2 $\mu\text{g}/\text{ml}$ nocodazole (Fig. 6C). The remaining panels in Figure 6 show these same experimental treatments, except that the cells were subsequently double-labeled for microtubules and Kif15. The lower latrunculin concentration resulted in the coalescence of some of the microtubules into dense bundles within the RFL-6 cells, but these microtubule bundles did not show any detectable co-localization with Kif15 (Fig. 6D) as did the microtubule bundles in neurons. This was also the case with the RFL-6 cells treated with the higher dose of latrunculin; dense microtubule bundles occupied the narrow processes but there was no enrichment of Kif15 within these bundles and no co-alignment with microtubules (Fig. 6E). The more stable, nocodazole-resistant microtubules showed no co-localization with Kif15 (Fig. 6F). Collectively these observations demonstrate that it is not possible to cause Kif15 to alter its distribution from one filament system to the other in RFL-6 cells by pharmacologically manipulating microtubules or F-actin.

Figure 7 shows similar pharmacologic studies on cultured sympathetic neurons grown on polylysine and then treated for 1–2 hrs with laminin prior to application of the drugs. Even the lowest concentration of latrunculin was effective in depleting any detectable F-actin staining in the neurons (Fig. 7A). The morphology of the latrunculin-treated neurons was altered somewhat from controls (Fig. 7A and B) with the axons appearing less straight and the lamellae somewhat collapsed. Kif15 continued to co-localize with microtubules (Fig. 7B), and continued to show a distal

Fig. 4. Kif15 and tubulin co-localize in cultured rat sympathetic neurons. Neurons were plated overnight on polylysine and not further treated with laminin or matrigel. (A) This neuron, which had extended only lamellae, was probed with anti-tubulin (left panel) and anti-Kif15 (middle panel). Arrows indicate an example of a microtubule (or small microtubule bundle) that is immunopositive for Kif15. Kif15 can be detected on some, but not all, microtubules. Right panel is the merged image (tubulin in red, Kif15 in green, overlay in yellow). (B, C) These neurons had extended short, show-growing axons. Commonly, neurons grown in this fashion have growth cones that intermittently stall, during which time they display tight knots of microtubules in the distal regions of the axons. (B) Neurons probed with anti-tubulin (left), and anti-Kif15 (middle); merge (right) of tubulin (red) and Kif15 (green). (C) Neurons probed with anti-actin (left), anti-Kif15 (middle); merge (right) of actin (red) and Kif15 (green). Staining for Kif15 and microtubules show a great deal of overlap, particularly in the regions where microtubules appear as bundles. No apparent co-localization with actin was detected. Arrows indicate examples of the distal enrichment of Kif15 frequently present in axons. The distal enrichment of Kif15 was observed in axons (and axonal branches) with stalled growth cones, but was not observed in distal regions of rapidly growing axons (and axonal branches) in which microtubules were more splayed apart (see middle growth cone of uppermost neuron in A). Bar, 25 μm (A); 20 μm (B, C).

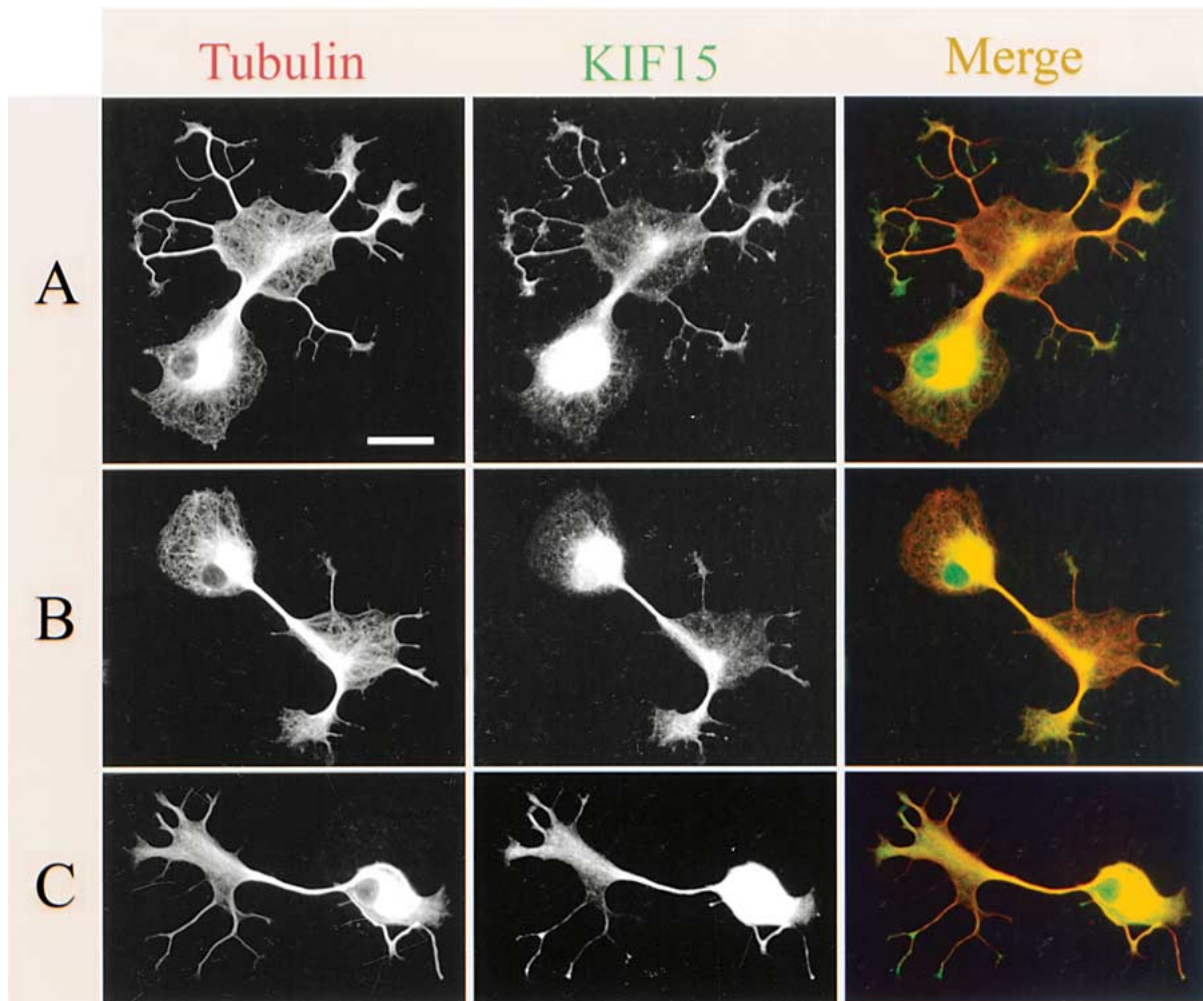


Fig. 5. Kif15 co-localizes with microtubules in rapidly growing neurons. Rat sympathetic neurons were exposed for 2 hrs to matrigel (A) or laminin (B, C) before fixation. Cultures were immunostained for tubulin (first column), and Kif15 (second column); merges are shown in the last column (tubulin in red, Kif15 in green, overlay in yellow). Staining for Kif15 and microtubules show a great deal of overlap, particularly in the regions where the microtubules appear as bundles. Growth cones stall less frequently when exposed to these growth factors, and more often display splayed microtubules in their distal regions; such splayed microtubules did not exhibit the particularly high enrichment for Kif15 that was observed within stalled growth cones.

enrichment in stalled growth cones (Fig. 7A). Treatment with nocodazole partially depolymerized the microtubules, causing a preferential loss of distal microtubules compared to those in the main-shaft region of

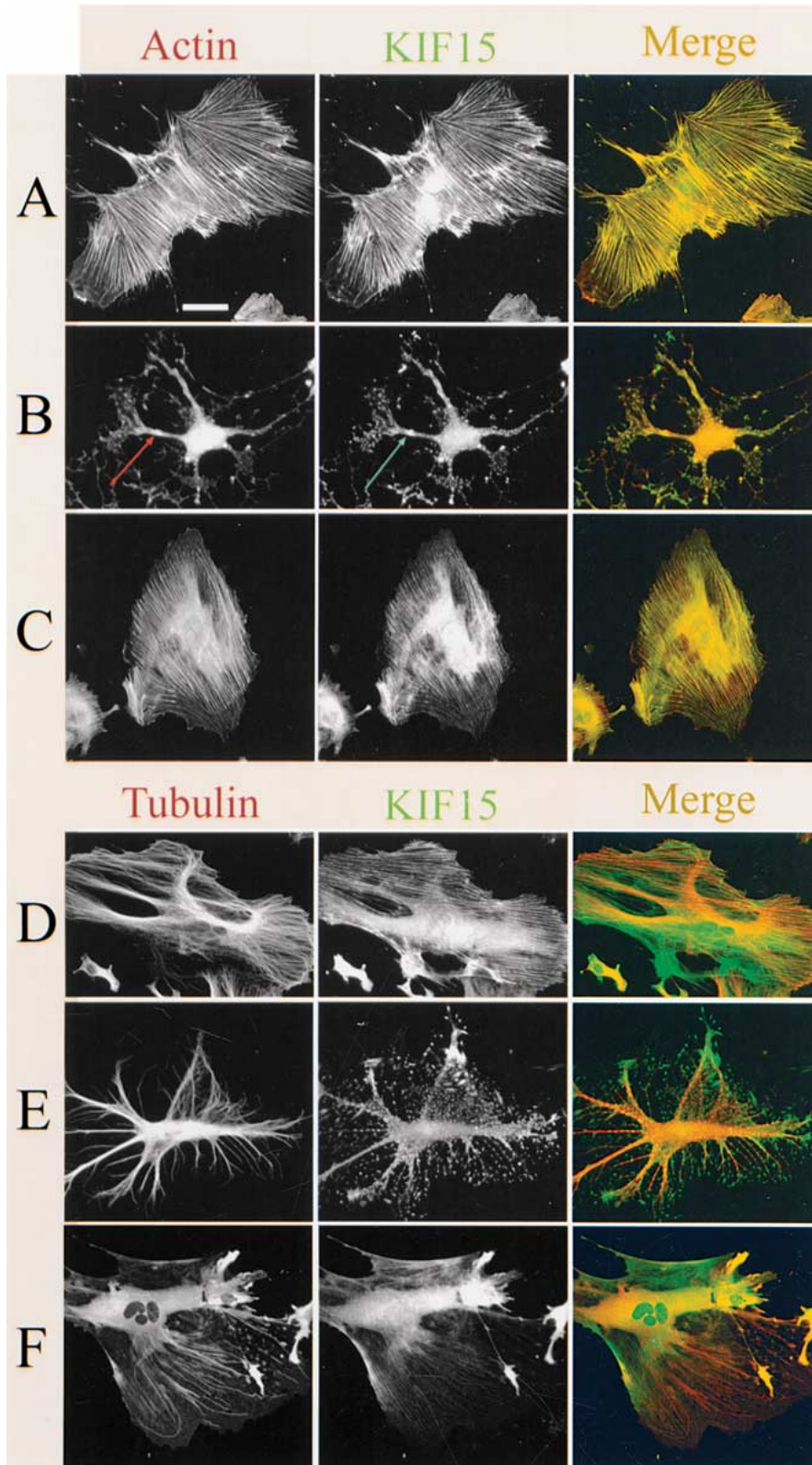
the axons (Fig. 7C). Kif15 continued to co-localize with the microtubules within the shafts of the axons. There was a clear loss of the distal Kif15 staining within stalled growth cones where microtubules were lost, and no

Fig. 6. Immunofluorescence of RFL-6 fibroblasts treated with latrunculin or nocodazole. (A, D) Treatment of RFL-6 cells with a low concentration of latrunculin spares microtubules (D, left panel) and denser actin bundles (A, left panel). Kif15 immunofluorescence co-localizes with actin bundles (A, middle and right panels) but not with microtubules (D, middle and right panels). Even the denser bundles of microtubules, which appear to be induced by the latrunculin treatment, do not co-localize with Kif15. Merged images (right panels): A, actin in red, Kif15 in green; D, microtubules in red, Kif15 in green; overlays in yellow. (B, E) Treatment with a high concentration of latrunculin causes a drastic change in cell morphology but preserves microtubules (E, left panel) while almost eliminating Kif15 and actin immunolocalization (middle panels and B, left panel). Arrows in B point to patches of remaining F-actin that continue to co-localize with Kif15, but microtubules do not co-localize with Kif15 as observed with neurons. Merged images (right panels): B, actin in red, Kif15 in green; E, microtubules in red, Kif15 in green; overlays in yellow. (C, F) Treatment of RFL-6 cells with nocodazole disassembles most microtubules (F, left panel) but does not detectably affect actin or Kif15 immunolocalization (C and F, middle panel). Bar, 50 μ m.

detectable Kif15 filamentous staining in the lamellar regions previously occupied by microtubules. Collectively, these results demonstrate that the characteristic distribution of Kif15 in neurons is microtubule- but not actin-dependent.

DISTRIBUTION OF Kif15 IN MATURING NEURONS AND DEVELOPING BRAIN

The studies described thus far demonstrate that Kif15 associates with microtubules in terminally postmitotic neurons, and that the association appears enhanced



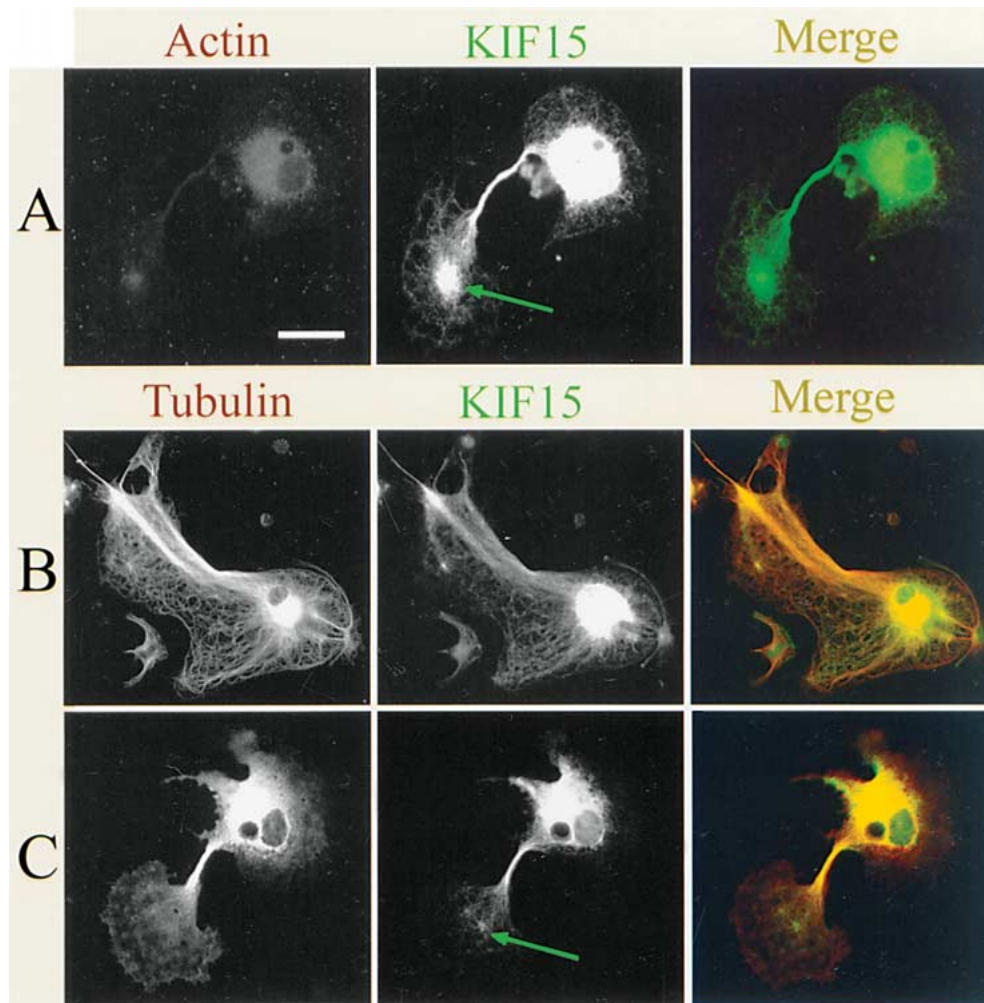


Fig. 7. Immunofluorescence of rat sympathetic neurons treated with latrunculin or nocodazole. (A) A low concentration of latrunculin abolishes the F-actin staining of the neurons (left panel) without loss of Kif15 immunofluorescence or localization (middle panel). Arrow indicates the distal enrichment of Kif15 frequently observed in axons with stalled growth cones. Merged image in right panel shows actin in red, Kif15 in green. (B) Microtubules remain after latrunculin treatment (left panel), and Kif15 immunostaining (middle panel) still closely corresponds to some microtubules. (C) Nocodazole disassembles much of the microtubule mass, particularly the more labile microtubules in the distal region of the axon and the lamellae extending from the cell body (left panel). Kif15 continues to co-localize with the microtubules remaining in the shaft of the axon, but no longer shows its typical pattern of staining in the regions of the neuron where microtubules are significantly depleted (middle panel). Arrow indicates the absence of Kif15 distal enrichment where microtubules have been depleted. (B, C) Right panels: actin in red, Kif15 in green, overlay in yellow. Bar, 20 μ m.

within regions of closely-packed microtubules compared to regions with individual unbundled microtubules. This conclusion is consistent with one of the proposed functions of Kif15 during mitosis, namely to crosslink neighboring microtubules and oppose the capacity of other motors to move them. To pursue this possibility further, we sought to determine if Kif15 is particularly enriched in certain compartments of more mature neurons, and if Kif15 is particularly enriched in certain neuronal populations in the developing brain. With regard to the first issue, we generated long-term cultures of rat sympathetic neurons, and then double-labeled them for Kif15 and tubulin to ascertain whether

dendrites contain different levels of Kif15 than axons. Dendrites are slower growing than axons and stop growing after reaching a certain length, and this appears to be due at least in part to motor forces that oppose the capacity of cytoplasmic dynein to move the microtubules as effectively as in axons (Yu *et al.*, 2000). Figure 8 shows neurons cultured for 6, 14, and 17 days. There are no dendrites apparent at 6 days, early dendrites at 14 days, and more robust dendrites at 17 days. The images shown in Figure 8 are ratio-images prepared on a Pascal confocal microscope and show the fluorescence ratio of Kif15 to tubulin, with lower ratios displayed in white, higher ratios in black, and

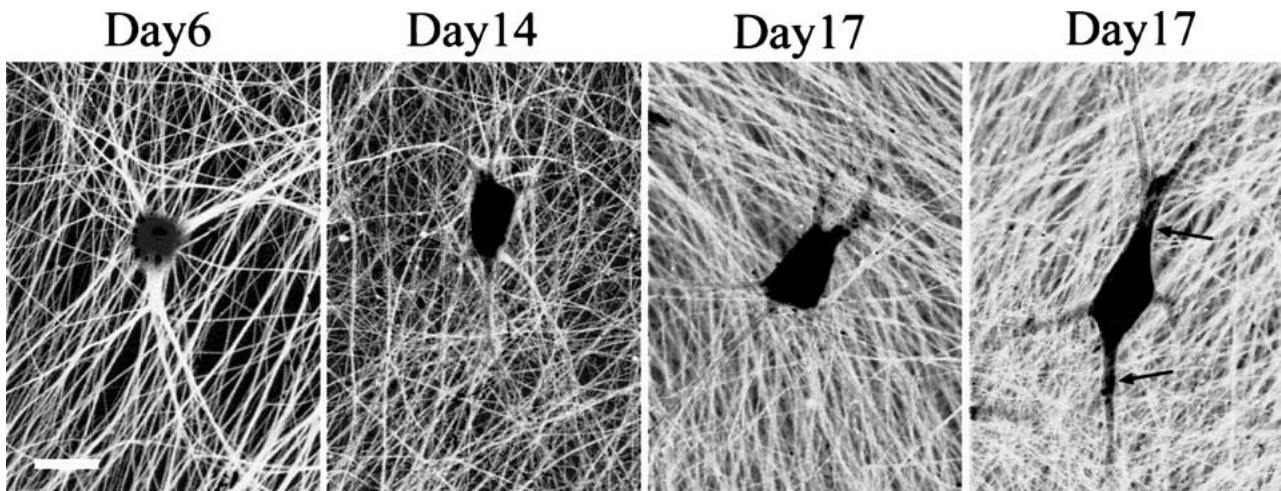


Fig. 8. Ratio images of Kif15 to tubulin in older cultures of sympathetic neurons. Rat sympathetic neurons were cultured for extended times to allow the development of dendrites. Images of the double immunolabeled neurons were digitally processed to produce ratio images which indicate the relative fluorescence intensities of Kif15 to tubulin as variable gray levels (black is high Kif15 to tubulin, white is low Kif15 to tubulin). Kif15 is dramatically enriched within dendrites as they appear (note black tone; arrows point to dendrites in the last panel). Cell bodies consistently have a high ratio at all stages of development. Bar, 30 μm .

intermediate ratios in shades of gray. The ratio of Kif15 to tubulin within the cell body is significantly higher than in the axon at all stages of development. Notably, as dendrites begin to appear, the dendrite ratio of Kif15 to tubulin begins to increase and approaches the ratio in the cell body by the time robust dendrites appear at day 17. Kif15 is present in both axons and dendrites, but is markedly more enriched in dendrites compared to axons.

Because the microtubules within migratory neurons appear to move in unison to “tow” the cell body, and because Kif15 apparently tethers microtubules during mitosis (see Introduction), we hypothesized that Kif15 titer might be particularly high in migratory neurons. To investigate this, we immunostained sectioned mouse brain for Kif15. Kif15 immunoreactivity is present in developing brain throughout embryonic and postnatal development, but is more highly expressed in specific regions. Postnatally, expression is most prominent in the external germinal layer (EGL) of the cerebellum (Fig. 9A and B). The external germinal layer is the source of granule cells and contains neurons in several stages of differentiation, including those that have recently migrated, and some that are still dividing, or growing axons, or about to migrate away from the EGL. A second layer of high Kif15 immunoreactivity deep to the EGL could be detected in early postnatal cerebellum at both P1 and P8. Both cells and processes in this second layer were immunoreactive, probably belonging to both Bergmann radial glia and granule cells migrating to their mature position in the internal granule layer, as well as granule cells that have recently arrived in the internal germinal layer. Dividing cells have not

been localized to this part of the cerebellar cortex. We performed *in situ* hybridization to confirm the Kif15 immunolocalization using an antibody-independent approach. The Kif15 hybridization and immunoreactivity distributions closely corresponded. This is readily apparent in P1 cerebellar cortex (Fig. 9C). Hybridization was observed in other brain regions where Kif15 immunoreactivity had been detected (data not shown). Kif15 immunoreactivity was expressed in other cells of the embryonic nervous system and was particularly prominent in radial glia, including their processes (data not shown).

As in cerebellum, Kif15 expression in other developing brain regions was often found where cells had recently divided and in cells that appeared to be migrating. For example, cells in ventricular zones and neighboring regions showed particularly high Kif15 immunoreactivity (Fig. 9E and F). The highest levels of immunoreactivity were in cells at some distance from ventricles and having the morphology of migrating cells (Fig. 9F). Cells associated with the rostral migratory stream were also highly Kif15-immunoreactive (Fig. 9G). The rostral migratory stream contains presumptive olfactory receptor neurons migrating from their germinal zones near ventricles towards the olfactory bulb.

To unequivocally confirm that Kif15-immunoreactive cells were neurons, we double-labeled sections from P8 mouse brain for Kif15 and β III-tubulin (a marker for post-mitotic neurons, Haendel *et al.*, 1996). In general, regions of proliferation showed high levels of Kif15, while surrounding regions showed high levels of β III-tubulin. In neighboring regions, however,

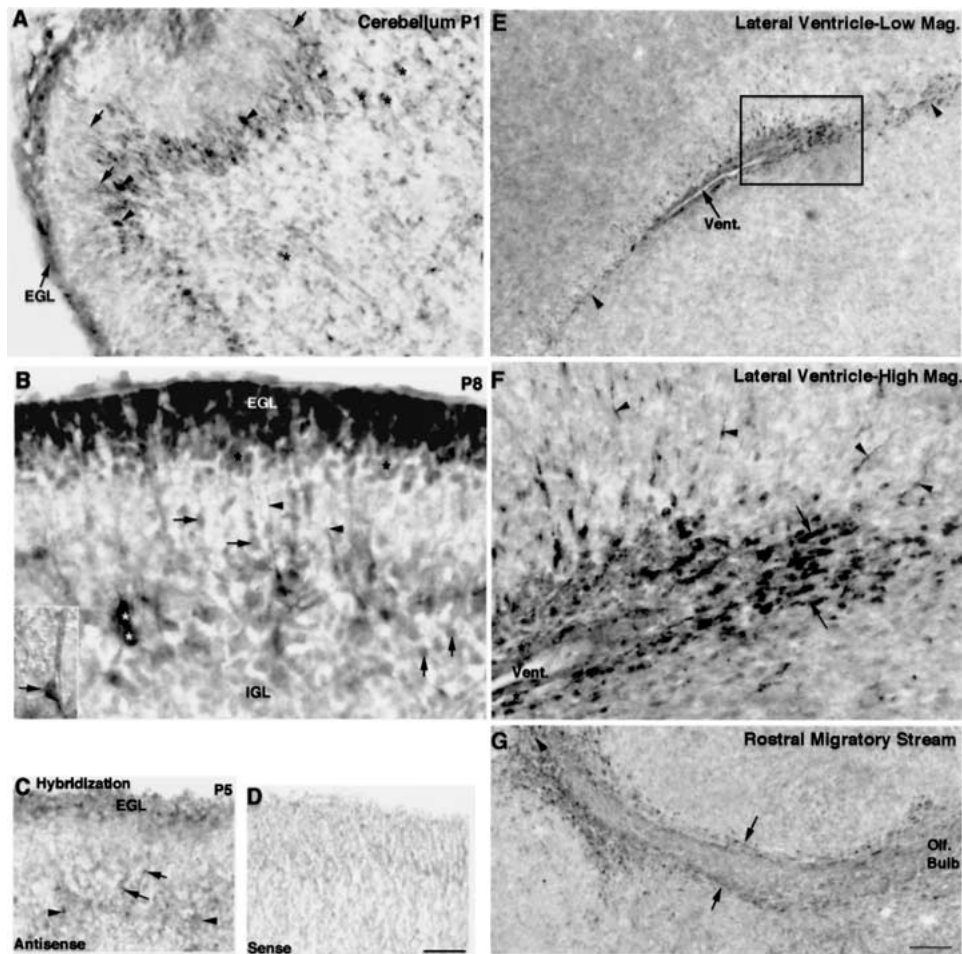


Fig. 9. Kif15 is enriched in mitotic neuronal precursors and migrating neurons in neonatal mouse brain. (A–D), Kif15 immunohistochemistry and *in situ* hybridization in neonatal mouse cerebellar cortex. (A) P1 cerebellum. Kif15-immunoreactivity is highest in the developing external germinal layer (“EGL”) that contains granule cell precursors. Immunoreactivity is also present in a deeper layer, both in cell bodies (arrowheads) and their superficially directed processes (arrows), probably belonging to Bergmann glia. Scattered immunoreactive cells are present in the presumptive internal granule layer (asterisks for examples). (B) P8 cerebellum, higher magnification. Cells in the superficial EGL have high levels of immunoreactivity, as do cell bodies (white asterisks) and processes (arrowheads) in the developing molecular and internal granule layers, probably corresponding to Bergmann glia or granule cells. Premigratory granule cells of the deeper EGL exhibit lower levels of immunoreactivity (black asterisks for examples), as do cells in the developing molecular and internal granule layers (arrows), which probably correspond to granule cells at various stages of their migration from EGL to IGL. Inset: High magnification DIC image of an immunoreactive cell in the molecular layer that has the form of a migratory granule cell with processes and is associated with a second process. (C) P5 cerebellum, Kif15 *in situ* hybridization. Many cells in the EGL possess Kif15 transcript, as do cells in a deeper layer (arrowheads), probably corresponding to Bergmann glia. Scattered Kif15-positive cells are located the EGL and in and around the deeper layer of expressing cells (arrows). (D) Control *in situ* hybridization, Kif15 sense probe. Little or no hybridization is detected using sense probe. (E–G) Kif15 immunohistochemistry, sagittal sections, P8 brain near lateral ventricle. (E) Immunoreactive cells are found adjacent to the ventricle (“Vent.”), and at a distance (arrowheads). (F) Boxed region in E at higher magnification. Immunoreactive cells are located adjacent to ventricle (asterisks), and at a distance (arrows), including cells in subventricular zones. Process-bearing cells further from ventricle are also immunoreactive (arrowheads). (G) Cells associated with the rostral migratory stream are Kif15-immunoreactive (between arrows). The olfactory bulb (right) is the destination of this stream. The ventricle is to the left (arrowhead) but outside the field of view. Bar, 40 μm (A, F); 20 μm (B); 13 μm (B, inset); 160 μm (C, D, E, G).

Kif15 and β III-tubulin co-localized in neurons. For example, Kif15 was highly expressed in the EGL of the cerebellum (Fig. 10B), while β III-tubulin was abundant in deeper layers (Fig. 10A). Cells near the Purkinje cell layer expressed both Kif15 and β III-tubulin (Fig. 10C).

Kif15 was high in many cells near ventricles (Fig. 10E), β III-tubulin was abundant further from the ventricle (Fig. 10D), and cells at intermediate distances expressed both Kif15 and β III-tubulin (Fig. 10D–F). In some brain regions, including the septum, process-bearing cells

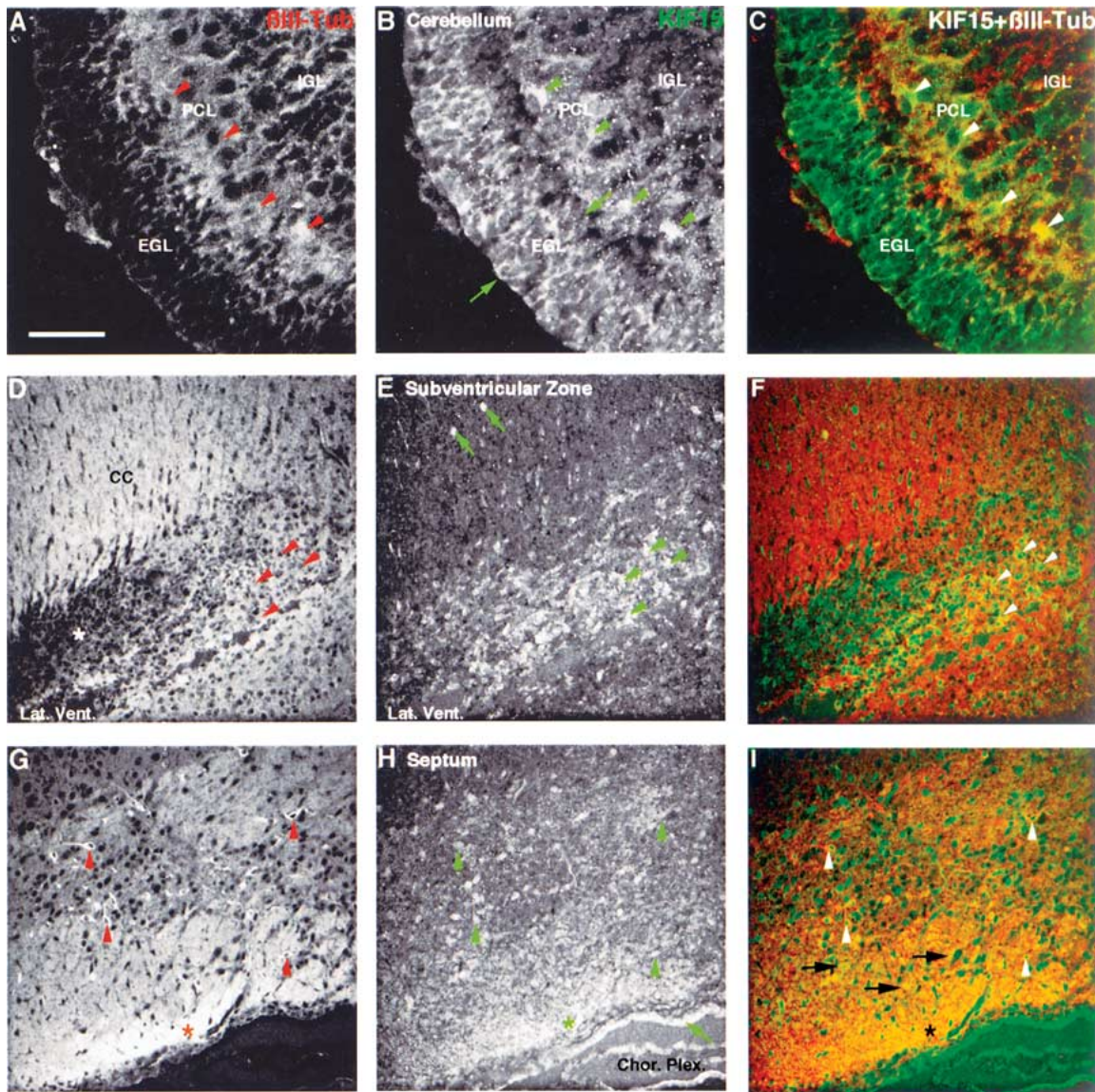


Fig. 10. Confocal images of double-label immunofluorescence for β III-tubulin (A, D, G), Kif15 (B, E, H) and the merged Kif15/ β III-tubulin images (C, F, I) in cerebellar cortex (A–C), a subventricular zone (D–F) and septum (G–I) from P8 mouse. (A) Cerebellum, β III-tubulin. Cells in the Purkinje cell layer (PCL) and the IGL are immunoreactive, while the superficial EGL has little immunoreactivity. Arrowheads indicate that cells near the PCL that have high Kif15 immunoreactivity (see B, C) are also β III-tubulin immunoreactive. (B) Same cerebellar section as (A), Kif15. Many cells in the EGL (between arrows) are highly immunoreactive, as are cells (arrowheads) near the PCL, probably Bergmann glia and some granule cells. (C) Same section as (A, B) Kif15 and β III-tubulin merge. Kif15 and β III-tubulin are co-localized in cells near the PCL (arrowheads). Cells in the superficial EGL express high levels of Kif15 (green), but little β III-tubulin (red), while cells of the IGL express less Kif15, and high levels of β III-tubulin. (D) Subventricular zone and surrounding regions, β III-tubulin. Although β III-tubulin is low in some regions (asterisk), many cells near the ventricle expressing high levels of Kif15 also express β III-tubulin (arrows). The axons of developing corpus colosum (“CC” and surrounding regions) are rich in β III-tubulin. (E) Same section as (D), Kif15. Many cells near the lateral ventricle (arrowheads) and more distant (arrows) are highly immunoreactive. (F) Same section as (D, E), Kif15 and β III-tubulin merge. Many cells and processes express either Kif15 (green) or β III-tubulin (red). Cells that express both Kif15 and β III-tubulin appear yellow or orange and are common in some regions (arrowheads for examples). (G) Septum, β III-tubulin. Little or no β III-tubulin is detected in choroid plexus, and in the cells that line the septum. (H) Same section as (G), Kif15. Cells of the choroid plexus and cells that line the surface of the septum (arrow) express high levels of Kif15. Processes and cell bodies at varying distances from the surface also show high levels of Kif15 (asterisk, arrowheads for examples). (I) Kif15 and β III-tubulin are co-localized (orange) in punctate structures probably representing processes both near the surface of the septum (asterisk) and in deeper regions (arrows). Kif15 and β III-tubulin are also co-localized in process-bearing cells, clearly visible in deeper regions of the septum (arrowheads). Comparisons with (H) indicate that Kif15 is present in the cytoplasm and processes of these cells, but is obscured by high levels of β III-tubulin labeling when they are both labeled. In (I) only the nuclei, which lack β III-tubulin, can clearly be seen to contain Kif15. Bar, 50 μ m (A–C); 25 μ m (D–G).

with the appearance of more mature neurons expressed both Kif15 and β III-tubulin (Fig. 10G–I).

Discussion

Microtubules can be highly dynamic, and there is abundant evidence suggesting that the microtubule arrays of various cell types are configured in large part by their dynamic assembly and disassembly. However, dynamics alone cannot explain the numerous microtubule behaviors that contribute to the formation of complex microtubule arrays such as those of mitotic spindles and terminally postmitotic neurons (Baas, 1999; Sharp *et al.*, 2000; Yu *et al.*, 2001). Motor-driven forces are known to play a critical role in the formation and function of the spindle (Sharp *et al.*, 2000; Wittmann *et al.*, 2001), and a growing body of evidence indicates that the same is true of neuronal microtubules (Baas, 1999). Live-cell imaging has directly revealed the movement of microtubules within the axonal shaft (Wang & Brown, 2002) as well as within regions of new growth at the distal tips and branch points of developing axons (Dent *et al.*, 1999). Inhibition studies from our laboratory indicate that forces generated by cytoplasmic dynein and CHO1/MKLP1 are essential for the proper distribution and configuration of microtubules within axons and dendrites (Sharp *et al.*, 1997; Ahmad *et al.*, 1998, 2000). Just as neurons contain a variety of factors that balance microtubule assembly and disassembly, it seems reasonable that they might also employ different motors to oppose as well as promote the movement of microtubules. In particular, there is evidence that the capacity of microtubules to move freely and independently of one another may be severely restricted in stalled growth cones, dendrites, and migratory neurons. Might a particular motor be crucial for this?

Recent studies have identified a kinesin-related motor which appears to function in this manner during mitosis. The activities of Xklp2 in frog and its homologue, KRP180, in sea urchin are not required to generate movement of microtubules during mitosis, but are required to maintain the separation of the half-spindles after other motors have moved them apart (Rogers *et al.*, 2000; Wittmann *et al.*, 2000, 2001). Xklp2 and KRP180 are believed to crosslink neighboring microtubules and exert forces that oppose the compressive forces that would otherwise collapse the bipolar spindle to a monastral array. In the present study, we have sought to identify the mouse and rat homologues of this family of motors, and to investigate their potential expression in terminally postmitotic neurons. The full-length sequences for the Xklp2 homologues (named Kif15) were obtained from rat brain, rat RFL-6 fibroblasts, and whole mouse embryos. Kif15 RNA from neonatal rat brain has virtually identical nucleotide sequence with the Kif15 transcript present in mitotically active rat RFL-6 cells, suggesting that the same Kif15 motor is present in both mitotic and

terminally post-mitotic cells. There was no evidence of splice variants in our studies, although there was an additional band of higher molecular weight on Western blots, which we suspect arises from an as yet unidentified posttranslational modification of Kif15. This band appears in both neurons and mitotic cells, suggesting that, whatever this modification, it is not a switch that distinguishes a neuronal and nonneuronal form of Kif15.

Studies on Xklp2 in M-phase *Xenopus* egg extracts, on KRP180 in mitotic sea urchin embryos, and on the human homologue Hklp2 in mitotic mammalian cells have demonstrated an association of the motor with spindle poles and microtubules from prometaphase to late anaphase (Boleti *et al.*, 1996; Rogers *et al.*, 2000; Sueishi *et al.*, 2000). Our antibodies replicated the published staining patterns when used to immunostain mitotically active RFL-6 cells. Kif15 was concentrated at spindle poles and on spindle microtubules prior to late anaphase, but Kif15 immunostaining of spindle microtubules was greatly reduced by late anaphase. By early cytokinesis, Kif15 immunolocalization was less intense on the microtubules, and most concentrated along the actin-rich, invaginating margins of dividing cells. Most interestingly, Kif15 does not co-localize with microtubules in interphase RFL-6 cells, but does display remarkably tight co-localization with actin filaments and bundles in roughly half the cells examined. Entirely similar observations were made on the fibroblastic nonneuronal cells that contaminate the sympathetic neuronal cultures (data not shown). In sharp contrast, the neurons within the sympathetic cultures showed no detectable co-localization with actin whatsoever, but showed good co-localization of a substantial portion of the microtubule array. Co-localization with microtubules was particularly good in regions where microtubules were tightly packed (and presumably bundled) rather than splayed apart. Thus, Kif15 distribution in postmitotic neurons reflected the pattern in fibroblasts in early mitosis rather than interphase, a finding reminiscent of other so-called mitotic proteins that we have studied in neurons (Baas, 1999; Ahmad *et al.*, 1999).

Even though it is apparently able to associate with either the actin or microtubule systems of fibroblasts, Kif15 is found exclusively on microtubules in terminally postmitotic neurons. A simple, but tenable, possibility is that Kif15 associates preferentially with the more abundant cytoskeletal system. During neurogenesis, the dense bundles of actin break down and give way to a finer actin cytoskeleton, much of which forms a cortical layer and a delicate cytomatrix along the length of the axon (Haendel *et al.*, 1996; Yu *et al.*, 2001). However, when the actin bundles and filaments in RFL-6 cells are disassembled with latrunculin, there is no detectable shift in the distribution of Kif15 to microtubules, not even to the denser bundles of microtubules. Other pharmacologic studies show that the association

of Kif15 with actin in the RFL-6 cells is not microtubule-dependent, nor is the association of Kif15 to microtubules in neurons actin-dependent. Studies with nocodazole confirm that the pattern of Kif15 distribution is microtubule-dependent within neurons. These pharmacologic studies demonstrate that the preference of Kif15 to associate with either microtubules or actin cannot be switched simply by depleting the other filament system.

The association of neuronal Kif15 with microtubules is not surprising, given that kinesins are microtubule-based motors. The fact that RFL-6 Kif15 can also associate with F-actin during certain cell cycle stages is consistent with our identification of a myosin-like tail domain within its sequence. We suspect that the myosin tail homology domain enables Kif15 to associate with myosin II within some actin fibers. Precedent for this scenario exists in the case of KhcU (the microtubule-binding heavy chain of mouse ubiquitous kinesin), which interacts with the actin-associated motor, MyoVA, by way of a myosin tail homology domain present in the KhcU stalk (Huang *et al.*, 1999). In terms of potential function, if the motor domains of the actin-associated Kif15 are still able to slide along microtubules, the forces would be expected to draw microtubules against the actin bundles toward the cell center, given that Kif15 is plus-end-directed. While this remains to be tested, there is precedent for functionally important interactions of other microtubule-based motors with actin. For example, a portion of dynein/dynactin in neurons is thought to interact with actin, and the resulting forces drive microtubules outward toward the cell periphery rather than inward (Ahmad *et al.*, 1998). Also, it has been shown that the kinesin-related motor CHO1 interacts directly with actin during the later stages of mitosis, and that this interaction is critical for the completion of cytokinesis (Kuriyama *et al.*, 2002). The manner by which Kif15 switches between microtubules and actin remains unknown, but we suspect that it might relate to the unique phosphorylation activities of neurons and cells in mitosis compared to cells in interphase.

The pattern and levels of Kif15 immunoreactivity in cultured neurons and brain are consistent with a neuronal function that is analogous to its mitotic function. Within neuronal lamellae and early axons, individual unbundled microtubules stain less consistently for Kif15 than microtubule bundles, which always show prominent staining. Kif15 levels are particularly high within stalled growth cones, which contain looped bundles of microtubules which show no apparent movement relative to one another until they splay apart (Dent *et al.*, 1999; Yu *et al.*, 2001); in dendrites, in which microtubule movements by cytoplasmic dynein are restricted by at least one other motor (Yu *et al.*, 2000); and in migratory neurons, in which a cage of microtubules surrounding the nucleus is somehow linked to

the microtubules within the leading process, such that the entire microtubule array moves as a crosslinked unit to drag the cell body (Rivas & Hatten, 1995; Feng & Walsh, 2001). Based on its properties and function in the spindle, it seems reasonable to conclude that Kif15 tethers the microtubules in these cases to restrict their independent movement. In the case of migratory neurons, the other motor-driven forces are still sufficient to move the microtubules, but do so by moving the entire microtubule array as a unit.

The means by which Kif15 opposes microtubule movements is unknown. During mitosis, Kif15 homologues have been proposed to immobilize the half-spindles by interacting with microtubules of opposite orientation (Rogers *et al.*, 2000). In neurons, Kif15 localizes to microtubule bundles of uniform polarity orientation as well as nonuniform orientation, but it is more enriched in regions where oppositely oriented microtubules overlap. Dendrites have nonuniformly oriented (anti-parallel) microtubules (Sharp *et al.*, 1995), while stalled growth cones contain bundles of uniformly oriented microtubules that loop back on themselves, thus generating overlapping microtubules of opposite orientation. The cage-like configuration of microtubules in migratory neurons has not been analyzed extensively with regard to microtubule polarity orientation, but would logically consist in part of interacting microtubules of opposite orientation. We cannot dismiss a potential role for Kif15 in attenuating microtubule movements within uniformly oriented arrays, however, given that Kif15 is present within axonal microtubule bundles and that microtubules in the axon spend most of their time pausing rather than moving (Wang *et al.*, 2002).

Acknowledgments

This work was supported by two grants from the National Institutes of Health to Peter W. Baas. Partial support for Daniel Buster and Wenqian Yu was provided by a training grant from the NIH. We thank Drs. Itzhak Fischer for advice and assistance.

References

- AHMAD, F. J., ECHEVERRI, C. J., VALLEE, R. B. & BAAS, P. W. (1998) Cytoplasmic dynein and dynactin are required for the transport of microtubules into the axon. *Journal of Cell Biology* **140**, 246–256.
- AHMAD, F. J., HUGHEY, J., WITTMANN, T., HYMAN, A., GREASER, M. & BAAS, P. W. (2000) Motor proteins regulate force interactions between microtubules and microfilaments in the axon. *Nature Cell Biology* **2**, 276–280.
- AHMAD, F. J., YU, W., MCNALLY, F. J. & BAAS, P. W. (1999) An essential role for katanin in severing microtubules in the neuron. *Journal of Cell Biology* **145**, 305–315.
- BAAS, P. W. (1999) Microtubules and neuronal polarity: Lessons from mitosis. *Neuron* **22**, 23–31.

- BOLETI, H., KARSENTI, E. & VERNOS, I. (1996) Xklp2, a novel *Xenopus* centrosomal kinesin-like protein required for centrosome separation during mitosis. *Cell* **84**, 49–59.
- DENT, E. W., CALLAWAY, J. L., SZEKENYI, G., BAAS, P. W. & KALIL, K. (1999) Reorganization and movement of microtubules in growth cones and developing interstitial branches. *Journal of Neuroscience* **9**, 8894–8904.
- DILLMANN III, J. F., DABNEY, L. P. & PFISTER, K. K. (1996) Cytoplasmic dynein is associated with slow axonal transport. *Proceedings of the National Academy Science USA* **93**, 141–144.
- FENG, Y. & WALSH, C. A. (2001) Protein-protein interactions, cytoskeletal regulation and neuronal migration. *Nature Reviews Neuroscience* **2**, 408–416.
- FERHAT, L., COOK, C., CHAUVIERE, M., HARPER, M., KRESS, M., LYONS, G. E. & BAAS, P. W. (1998) Expression of the mitotic motor protein Eg5 in postmitotic neurons: Implications for neuronal development. *Journal of Neuroscience* **18**, 7822–7835.
- HAENDEL, M. A., BOLLINGER, K. E. & BAAS, P. W. (1996) Cytoskeletal changes during neurogenesis in cultures of avian neural crest cells. *Journal of Neurocytology* **25**, 289–301.
- HATTEN, M. E. (1999) Central nervous system neuronal migration. *Annual Review of Neuroscience* **22**, 511–539.
- HE, Y. & BAAS, P. W. (2003) Growing and working with peripheral neurons. In *Nerve Cell Biology* (edited by HOLLENBECK, P. & BAMBURG, J.), a volume in *Methods in Cell Biology* **71**, 17–35.
- HUANG, J.-D., BRADY, S. T., RICHARDS, B. W., STENOLEN, D., RESAU, J. H., COPELAND, N. G. & JENKINS, N. A. (1999) Direct interaction of microtubule- and actin-based transport motors. *Nature* **397**, 267–270.
- KURIYAMA, R., GUSTUS, C., TERADA, Y., UETAKE, Y. & MATULIENE, J. (2002) CHO1, a mammalian kinesin-like protein, interacts with F-actin and is involved in the terminal phase of cytokinesis. *Journal of Cell Biology* **156**, 783–790.
- NAKAGAWA, T., TANAKA, Y., MATSUOKA, E., KONDO, S., OKADA, Y., NODA, Y., KANAI, Y. & HIROKAWA, N. (1997) Identification and classification of 16 new kinesin superfamily (KIF) proteins in mouse genome. *Proceedings of the National Academy Science USA* **94**, 9654–9659.
- RIVAS, R. J., BURMEISTER, D. W. & GOLDBERG, D. J. (1992) Rapid effects of laminin on the growth cone. *Neuron* **8**, 107–115.
- RIVAS, R. J. & HATTEN, M. E. (1995) Motility and cytoskeletal organization of migrating cerebellar granule neurons. *Journal of Neuroscience* **15**, 981–989.
- ROGERS, G. C., CHUI, K. K., LEE, E. W., WEDAMAN, K. P., SHARP, D. J., HOLLAND, G., MORRIS, R. L. & SCHOLEY, J. M. (2000) A kinesin-related protein, KRP180, positions prometaphase spindle poles during early sea urchin embryonic cell division. *Journal of Cell Biology* **150**, 499–511.
- SAMBROOK, J., FRITSCH, E. F. & MANIATIS, T. (1989) *Molecular Cloning. A Laboratory Manual*. 2nd edition. Cold Spring Harbor Laboratory Press.
- SHARP, D. J., ROGERS, G. C. & SCHOLEY, J. M. (2000) Microtubule motors in mitosis. *Nature* **407**, 41–47.
- SHARP, D. J., YU, W. & BAAS, P. W. (1995) Transport of dendritic microtubules establishes their nonuniform polarity orientation. *Journal of Cell Biology* **130**, 93–104.
- SHARP, D. J., YU, W., FERHAT, L., KURIYAMA, R., RUEGER, D. C. & BAAS, P. W. (1997) Identification of a microtubule-associated motor protein essential for dendritic differentiation. *Journal of Cell Biology* **138**, 833–843.
- SLAUGHTER, T. S., WANG, J. & BLACK, M. M. (1997) Transport of microtubules from the cell body into the axons of cultured neurons. *Journal of Neuroscience* **17**, 5807–5819.
- SMITH, D. S., NIETHAMMER, M., AYALA, R., ZHOU, Y., GAMBELLO, M. J., WYNshaw-BORIS, A. & TSIA, L.-H. (2000) Regulation of cytoplasmic dynein behavior and microtubule organization by mammalian Lis1. *Nature Cell Biology* **2**, 767–775.
- SUEISHI, M., TAKAGI, M. & YONEDA, Y. (2000) The forkhead-associated domain of Ki-67 antigen interacts with the novel kinesin-like protein Hklp2. *Journal of Biological Chemistry* **275**, 28888–28892.
- TRENKNER, E. (1991) Cerebellar cells in culture. In *Culturing Nerve Cells* (edited by BANKER, G. & GOSLIN, K.) pp. 283–307. MIT Press.
- TANG, D. & GOLDBERG, D. J. (2000) Bundling of microtubules in the growth cone induced by laminin. *Molecular and Cellular Neuroscience* **15**, 303–313.
- WANG, L. & BROWN, A. (2002) Rapid movement of microtubules in axons. *Current Biology* **12**, 1496–1501.
- WITTMANN, T., HYMAN, A. & DESAI, A. (2001) The spindle: A dynamic assembly of microtubules and motors. *Nature Cell Biology* **3**, E28–E34.
- WITTMANN, T., WILM, M., KARSENTI, E. & VERNOS, I. (2000) TPX2, a novel *Xenopus* MAP involved in spindle pole organization. *Journal of Cell Biology* **149**, 1405–1418.
- WYNshaw-BORIS, A. & GAMBELLO, M. J. (2001) LIS1 and dynein motor function in neuronal migration and development. *Genes & Development* **15**, 639–651.
- YU, W., AHMAD, F. J. & BAAS, P. W. (1994) Microtubule fragmentation and partitioning in the axon during collateral branch formation. *Journal of Neuroscience* **14**, 5872–5984.
- YU, W., COOK, C., KURIYAMA, R., KAPLAN, P. L. & BAAS, P. W. (2000) Depletion of a microtubule-associated motor protein induces the loss of dendritic identity. *Journal of Neuroscience* **20**, 5782–5781.
- YU, W., LING, C. & BAAS, P. W. (2001) Microtubule reconfiguration during axogenesis. *Journal of Neurocytology* **30**, 861–875.
- YU, W., SCHWEI, M. J. & BAAS, P. W. (1996) Microtubule transport and assembly during axon growth. *Journal of Cell Biology* **133**, 151–157.